Journal of Hazardous Materials 514 (2026) 142913

Contents lists available at ScienceDirect

Journal of Hazardous Materials

journal homepage: www.elsevier.com/locate/jhazmat

A short-trip combination method for reconstructing real-world NOx emission indicators from irregular OBD telematics of heavy-duty diesel vehicles

Chuntao Liu [a], Chenxi Wang [b,*], Zhiqiang Li [a], Dasuo Yao [a], Yiqiang Pei [a,c], Chunling Wu [d]

[a] *School of Mechanical Engineering, Tianjin Renai College, Tianjin 300392, China*
[b] *Institute for Transport Studies, University of Leeds, Leeds LS2 9JT, UK*
[c] *State Key Laboratory of Engines, Tianjin University, Tianjin 300072, China*
[d] *CATARC Automotive Test Center Company Limited, Tianjin 300399, China*

HIGHLIGHTS

- STCM reconstructs MAW-based NOx indicators from irregular OBD data.
- The method was developed using 502 heavy-duty vehicles and 1.7 million trips.
- A 51-h window and 200 iterations yielded stable indicator estimates.
- STCM agreed with repeated PEMS results within 0.11–0.20 g/kWh.
- The method supports fleet-scale screening of in-use NOx emissions.

GRAPHICAL ABSTRACT

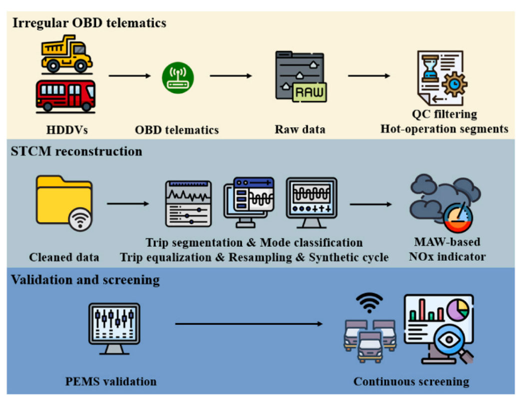

ARTICLE INFO

Keywords:
NOx emissions
Onboard diagnostics
Heavy-duty diesel vehicles
Telematics
Emission reconstruction

ABSTRACT

Heavy-duty diesel vehicles remain an important in-use source of atmospheric NOx, yet long-duration characterization of real-world emissions is constrained by the cost of Portable Emission Measurement Systems (PEMS) and by the irregular structure of Onboard Diagnostics (OBD) telematics. Using 13 months of 1 Hz telematics data from 502 China VI heavy-duty diesel vehicles, covering approximately 1.7 million trips, this study developed a Short-Trip Combination Method (STCM) to reconstruct a screening-oriented estimate of the 90th-percentile Moving Average Window (MAW) specific NOx emission indicator for hot-running operation. STCM segments thermally stabilized operation into short trips, classifies trips by driving mode, reconstructs regulation-constrained synthetic cycles through Monte Carlo resampling, and then calculates the MAW-based NOx indicator. The framework was benchmarked against 15 PEMS tests on four representative vehicles and further compared with a simple whole-trip averaging baseline. A 51-h evaluation window and 200 Monte Carlo iterations provided stable estimates. Median STCM estimates fell within the range of repeated PEMS measurements, with vehicle-level absolute errors of 0.11–0.182 g/kWh, whereas the supplementary baseline comparison showed

* Corresponding author.
E-mail address: c.wang2@leeds.ac.uk (C. Wang).

https://doi.org/10.1016/j.jhazmat.2026.142913
Received 16 April 2026; Received in revised form 3 June 2026; Accepted 5 July 2026
Available online 9 July 2026

lower agreement for whole-trip averaging. These results indicate that irregular long-duration OBD data can be converted into environmentally relevant hot-running NOx indicators that recover persistent elevated-emission behavior under real-world operation. Rather than replacing regulatory PEMS testing, the proposed framework provides a practical basis for continuous fleet-scale screening and prioritization of vehicles or operating periods requiring confirmatory inspection.

1. Introduction

Global economic expansion and accelerating urbanization continue to increase demand for freight and passenger transport, thereby intensifying environmental pressures from mobile-source emissions. The transportation sector is a major contributor to nitrogen oxides (NOx) emissions across many economies. For instance, in the 27 European Union member states, this sector was responsible for a substantial 56.5% of total NOx emissions in 2022 [1]. Within road transport, the influence of Heavy-Duty Diesel Vehicles (HDDVs) is particularly pronounced. Although HDDVs constitute only a small fraction of the total vehicle fleet, they account for a disproportionate share of on-road NOx emissions [2]. Because of their high engine loads, long activity durations, and frequent operation in freight and passenger corridors, HDDVs remain important contributors to roadside and urban NOx burdens. The hazardous relevance of HDDV NOx emissions is particularly pronounced in urban corridors, where frequent acceleration, congestion, and high engine load occur close to exposed populations. NOx promotes photochemical ozone formation and participates in secondary nitrate aerosol formation, thereby linking in-use diesel activity to both regional oxidant pollution and fine-particle burdens [3].

Although zero-emission heavy-duty vehicle technologies are advancing, diesel HDDVs are likely to remain a substantial in-use source of atmospheric NOx in the near term because fleet turnover is slow and large legacy fleets remain in service [4,5]. Selective Catalytic Reduction (SCR) is the principal technology for controlling NOx emissions from modern heavy-duty diesel vehicles and can achieve high conversion efficiency under well-controlled thermal conditions. However, in-use NOx emissions remain strongly influenced by transient driving conditions, traffic congestion, thermal management, and the in-use condition of the after-treatment system [6,7].

A substantial body of evidence indicates that real-world NOx emissions frequently exceed certification levels. For example, tests on 2010-model-year HDDs in the United States revealed real-world urban-cycle NOx emissions 2–3.5 times higher than the certified standards [8]. Similar phenomena have been documented in studies across China [9] and Europe [10]. Furthermore, malfunction, deterioration, or tampering of after-treatment systems can lead to substantial emission increases [11]. These observations indicate that long-duration characterization of in-use NOx behavior remains essential for environmentally relevant assessment of heavy-duty vehicle emissions.

Current approaches to in-use emissions monitoring each face important limitations in scalability, cost, or temporal representativeness. Laboratory chassis dynamometer testing cannot fully replicate the transient characteristics of real-world driving and is therefore unsuitable for timely fleet-scale monitoring [12,13]. Portable Emission Measurement Systems (PEMS) provide reference-grade real-world emissions data, yet their cost and operational complexity limit routine deployment across large fleets [14,15]. Remote sensing provides only instantaneous snapshots and is sensitive to plume dispersion and meteorological conditions, which limits its ability to characterize long-duration emission behavior [16,17]. Emission models support large-scale extrapolation, but often yield substantial errors in predicting emissions from individual vehicles because of simplified representations of engine operation and after-treatment dynamics [18,19]. Consequently, a practical need remains for a monitoring framework that combines environmental relevance, robustness, and fleet-scale applicability.

In recent years, the proliferation of the Internet of Things (IoT) and telematics has enabled remote monitoring technologies based on On-board Diagnostics (OBD), providing a new data source for characterizing in-use vehicle emissions [20]. Leveraging OBD telematics data, prior studies have developed real-time monitoring platforms and machine-learning approaches to identify high emitters or estimate on-road NOx emissions [21,22]. The China VI regulation requires HDDVs to be equipped with remote monitoring terminals that transmit key engine and after-treatment parameters at 1 Hz [23], thereby generating large volumes of real-world operational data. However, current telematics practice remains data-rich but information-poor for environmental assessment: large amounts of routine data are collected, but their fragmented and irregular structure prevents direct interpretation using the established China VI/RDE PEMS Moving Average Window (MAW) reference framework [24,25].

The MAW method was developed for continuous, structured test cycles with prescribed phase order, defined start and end points, and window-validity constraints. Real-world telematics, by contrast, consist of fragmented trip sequences with arbitrary stop-start events, variable durations, and intermittent engine-off periods. Therefore, the challenge addressed here is not primarily sensor precision or data transmission, although both remain important sources of uncertainty. The central methodological gap is the structural mismatch between stochastic routine operation and the standardized MAW interpretation framework [26,27]. Existing OBD-based studies have often relied on simplified approaches, such as whole-trip averaging or methods that do not fully apply MAW validity criteria, which are useful for rapid estimation but do not resolve this structural mismatch [28].

Against this background, the key challenge is not merely to estimate in-use NOx emissions from telematics, but to reconstruct a stable long-duration indicator from fragmented routine operation while preserving interpretability against a reference window-based framework. The present study addresses this challenge by developing and validating the Short-Trip Combination Method (STCM). The study makes three contributions. First, it proposes a cycle-reconstruction strategy that converts fragmented real-world operation into synthetic cycles suitable for stable MAW-based indicator reconstruction. Second, using telematics data from 502 China VI heavy-duty vehicles, it identifies practical conditions for fleet-scale implementation, including the required evaluation-window length and Monte Carlo sample size. Third, through comparison with repeated PEMS tests, it evaluates whether long-duration irregular OBD data can recover environmentally relevant elevated-emission behavior with sufficient agreement for screening use. Although the empirical setting is China VI, the broader methodological contribution lies in improving the environmental usefulness of routine digital monitoring for long-duration reconstruction of in-use NOx emissions.

2. Methodology

2.1. Data acquisition

The raw data used in this study were obtained from a HDDV remote monitoring platform compliant with the China VI technical requirements (GB 17691–2018). The dataset comprised telematics records from 502 HDDVs collected over a 13-month period, encompassing approximately 1.7 million individual trips. The fleet covered vehicle categories from M1 to N3 (except N1), with M3 passenger vehicles and N3 goods vehicles dominating the sample. As shown in Fig. 1, these two

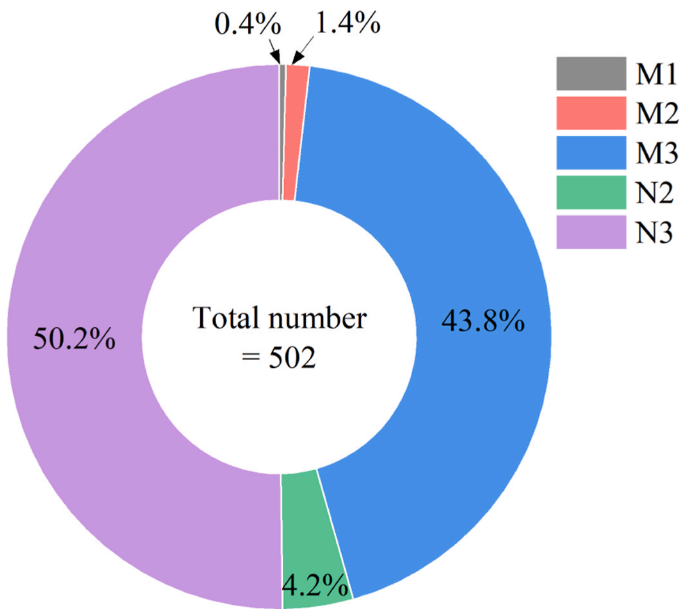

Fig. 1. Distribution of vehicle categories within the study fleet.

categories accounted for most of the fleet, while N2 and M1 vehicles represented smaller fractions. The vehicles covered a broad range of engine displacements (4.5–12.8 L) and rated powers (140–350 kW), and all were equipped with China VI-compliant after-treatment systems. This fleet structure provides a suitable basis for developing a fleet-screening method, although category-specific validation remains necessary for less represented groups such as N2 vehicles.

Data acquisition adhered strictly to the specifications of the China VI emission standard. Twenty critical parameters were recorded and uploaded at a frequency of 1 Hz. These parameters include essential variables for emission modeling and vehicle activity analysis, such as vehicle speed, engine torque and speed, fuel flow rate, and NOx concentrations upstream and downstream of the SCR catalyst. A complete list of parameters is provided in Table 1. Before analysis, the raw telematics data were subjected to rule-based quality control. Records were removed if they contained duplicated timestamps, invalid GPS status, physically implausible values, or prolonged signal interruption. The exact filtering criteria are now listed in Supplementary Table S1, including the time-gap threshold for prolonged interruption, valid ranges for NOx concentration, vehicle speed, engine speed, coolant temperature, and consistency checks for fuel-flow and torque-related signals.

Table 1
Remote monitoring data parameters (compliant with China VI standard).

ID	Parameter	Unit	ID	Parameter	Unit
1	Timestamp	-	11	Air Flow Rate	kg/h
2	Vehicle Speed	km/h	12	SCR Upstream Temperature	°C
3	Atmospheric Pressure	kPa	13	SCR Downstream Temperature	°C
4	Engine Net Torque	%	14	DPF Differential Pressure	kPa
5	Engine Friction Torque	%	15	Engine Coolant Temperature	°C
6	Engine Speed	r/min	16	Fuel Level	%
7	Engine Fuel Flow Rate	L/h	17	GPS Status	-
8	SCR Upstream NOx Sensor Output	10^{-6}	18	Longitude	°
9	SCR Downstream NOx Sensor Output	10^{-6}	19	Latitude	°
10	DEF (Urea) Level	%	20	Cumulative Mileage	km

2.2. Reference PEMS testing protocol

For proof-of-concept benchmark validation of the STCM, four vehicles were selected from the main fleet to represent distinct duty cycles and operating patterns, including one N3 goods vehicle and three M3 passenger vehicles. These vehicles cannot statistically represent the full emission diversity of the 502-vehicle fleet; therefore, the PEMS comparison is interpreted as benchmark validation of method feasibility rather than universal fleet-level validation. The selected vehicles nevertheless cover the dominant N3 and M3 categories and contrasting vocations in the dataset, including variable-route freight service, structured commuter-bus operation, and more variable tourism-related bus service. Vehicle A (N3 truck) primarily transports steel products between Tianjin and Beijing and typically operates under high-load, variable-route conditions. Vehicles B and C (M3 buses) operate as commuter shuttles along fixed urban routes with regular stop-start patterns. Vehicle D (M3 bus) provides scheduled tourist services within the Tianjin metropolitan area, with passenger load varying by seasonal tourism demand and weather conditions. All four vehicles are equipped with modern DOC-DPF-SCR-ASC after-treatment systems compliant with China VI emission standards. Their specifications are presented in Table 2, photographs are shown in Fig. 2, and their representativeness relative to the broader fleet is summarized in Supplementary Table S5.

All PEMS validation tests were conducted in strict accordance with the RDE test procedures mandated by the China VI standard. Tests were performed on public roads under ambient temperatures ranging from 15 to 25 °C. RDE routes were designed to comply with regulatory requirements regarding trip composition and distance. Following the RDE requirements specified in Appendix K of the China VI standard GB 17691–2018 [29], the target shares of urban, rural, and motorway operation were 20% ± 5%, 25% ± 5%, and 55% ± 5%, respectively, for Vehicle A as an N3 goods vehicle. For the M3 passenger buses (Vehicles B, C, and D), the corresponding target shares were 45% ± 5%, 25% ± 5%, and 30% ± 5%, respectively, unless a vehicle is formally classified as an urban vehicle, for which the China VI protocol specifies 70% urban and 30% rural operation. All tests followed the prescribed order of urban, rural, and motorway driving. NOx concentrations in the tailpipe exhaust were measured using a reference-grade PEMS (AVL M.O.V.E. GAS PEMS 493). The system configuration is illustrated in Fig. 3, and its key performance specifications are summarized in Table 3. To capture the inherent variability of real-world testing, each vehicle underwent three to four replicate RDE tests under similar but non-identical traffic and road conditions.

2.3. Reference window-based NOx indicator calculation

This study adopts the MAW method as the reference algorithm for

Table 2
Vehicle specifications for remote monitoring subjects.

Parameter	Vehicle A	Vehicle B	Vehicle C	Vehicle D
Vehicle Type	Goods Truck	Passenger Bus	Passenger Bus	Passenger Bus
Vehicle Category	N3	M3	M3	M3
Gross Vehicle Weight (kg)	25000	11850	11850	16700
Rated Engine Power (kW)	199	169	169	220
Rated Engine Speed (r/min)	2300	2200	2200	2200
Engine Displacement (L)	6.2	5.1	5.1	7.8
Aftertreatment System	DOC + DPF + SCR + ASC (China VI compliant)			

Fig. 2. Photographs of vehicles used for PEMS benchmark validation.

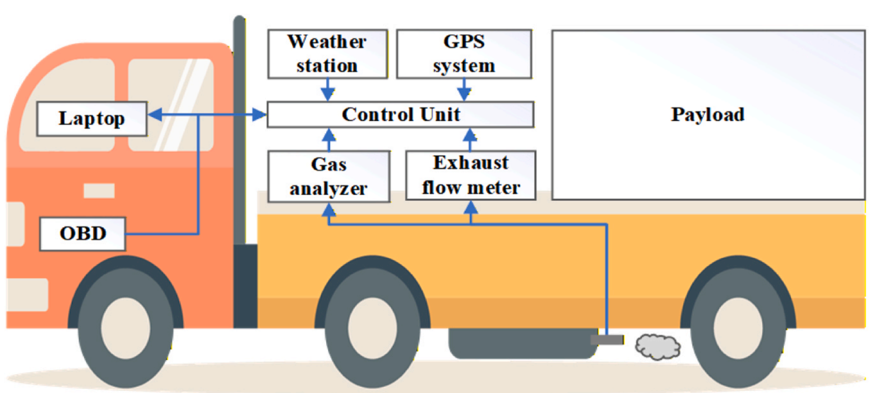

Fig. 3. Schematic diagram of PEMS equipment installed on board for RDE testing.

Table 3
Key specifications of the AVL M.O.V.E. GAS PEMS 493 analyzer.

Parameter	Specification
Operating Temperature Range	−30–45 °C
Measurement Range	NO: 0–0.5 vol%, NO_2: 0–0.25 vol%
Zero Point Drift	NO, NO_2: 2× 10^{-4} vol% / 8 h
Drive Voltage	24 V DC
Total System Weight	~50 kg

calculating route-specific NOx emissions and reconstructing a benchmark window-based NOx indicator. Given the inherent variability in real-world driving, RDE test repeatability is affected by route, traffic, driver behavior, and ambient conditions. The MAW method reduces part of this variability by segmenting continuous emission data into engine-work-based windows, thereby extracting a comparable metric across diverse driving patterns [26]. A window is defined as a subset of test data beginning after the engine coolant temperature first exceeds 70 °C. The window ends when the accumulated engine work reaches the reference value Wref, namely the total work of the World Harmonized Transient Cycle (WHTC). Subsequent windows are generated by shifting the start point forward by 1 s, providing comprehensive coverage of the hot-running part of the test, as depicted in Fig. 4.

Cumulative work is calculated from Controller Area Network (CAN) parameters using Eq. (1). Instantaneous engine power was derived from engine speed and brake torque reconstructed from the OBD-reported net torque and friction torque signals together with the manufacturer-reported reference torque under the China VI data definition.

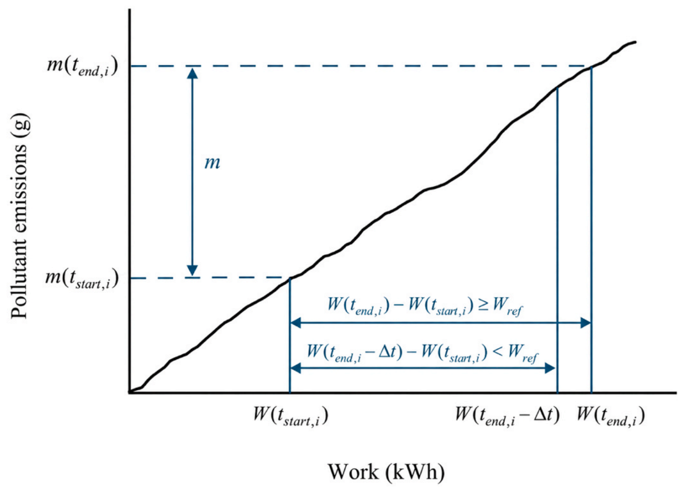

Fig. 4. Schematic diagram of the MAW method.

$$W = \frac{1}{3600}\int_{t_{1,i}}^{t_{2,i}} Pwdt = \frac{1}{3600}\int_{t_{1,i}}^{t_{2,i}} \frac{Tq \times n_e}{9549}dt \quad (1)$$

where W is the cumulative engine work (kWh) over the window, Pw is the instantaneous engine power (kW), Tq is the engine output torque (N·m), and n_e is the engine speed (r/min).

The instantaneous NOx mass emission rate $\dot{m}_{NOx}$ (g/s) is calculated using Eq. (2). Exhaust mass flow rate was estimated from the telematics-reported intake-air flow and fuel-flow signals under the assumption of mass conservation, with unit conversion and density correction applied consistently throughout the analysis.

$$\dot{m}_{NOx} = \frac{c_{NOx} \times 10^{-6} \times \dot{m}_{exh} \times \frac{1000}{3600} \times M_{NOx}}{22.4 \times 10^{-3} \times \rho \times 10^3} = 4.412 \times 10^{-7} \times c_{NOx} \times \dot{m}_{exh} \quad (2)$$

Where $\dot{m}_{exh}$ represents the exhaust mass flow rate (kg/h), c_{NOx} is the NOx concentration (10^{-6}), M_{NOx} is the molar mass of NOx (46 g/mol), and ρ is the density of air under standard conditions (1.293 kg/m^3), with the numerical constant derived from these fundamental physical constants.

The resulting window-specific NOx metric (SE_{NOx}, in g/kWh), is then calculated using Eq. (3).

$$SE_{NOx} = \frac{m_{NOx}}{W} \quad (3)$$

Where m_{NOx} is the cumulative NOx mass (g) emitted within the window.

A critical aspect of the MAW method is the validation of individual windows. A window-specific SE_{NOx} value is considered valid for final indicator calculation only if the window average power ratio (APR) exceeds a predefined power threshold [29]. APR is defined as the ratio of the average power within the window to the engine maximum rated power, as expressed in Eq. (4).

$$APR = \frac{Pw_{avg}}{Pw_{max}} \times 100\% \quad (4)$$

.

In standard RDE testing protocols, the initial power threshold is conventionally set to 20% of the engine maximum power. If valid windows account for less than 50% of all windows generated from the test data, the power threshold is iteratively reduced in 1% increments until the valid-window proportion reaches at least 50%. If the threshold would fall below an absolute minimum of 10%, the test is deemed invalid for compliance assessment. For a valid test, the final NOx indicator is the 90th percentile of the specific NOx emissions calculated from all valid windows (SE_{NOx}_P90). Under the China VI standard, $SE_{NOx}\_P90 <= 0.69$ g/kWh is specified for regulatory interpretation [29]. In the present study, this value is used only as a reference benchmark for screening-oriented interpretation, not as a formal compliance decision criterion.

2.4. STCM framework for real-world NOx indicator reconstruction

The implementation proceeds through four sequential stages, as illustrated in Fig. 5. Stage 1 performs data preprocessing and initial trip segmentation. Raw OBD data are cleaned using the quality-control rules in Supplementary Table S1. The cleaned data stream is then segmented using idle periods as initial boundaries. Because the telematics stream is recorded at 1 Hz, an idle interval of at least 1 s is the minimum observable zero-speed event and is therefore used only as the initial boundary-detection rule. This rule intentionally preserves stop-and-go micro-dynamics in congested operation. To avoid allowing micro-trips to dominate Monte Carlo sampling, these initial fragments are subsequently standardized through same-mode merging and long-trip splitting, as described in Supplementary Table S2. All data points recorded when the engine coolant temperature is below 70 °C are excluded from the hot-running indicator calculation, keeping the reconstructed indicator comparable with the China VI/RDE MAW evaluation boundary.

Stage 2 performs trip classification and length equalization. Each segmented hot trip is classified as urban, rural, or motorway according to the applicable China VI speed thresholds. The initial segmentation commonly produces a highly uneven duration distribution: urban congestion generates many very short fragments, whereas rural and motorway operation often produces long continuous fragments. To avoid excessive dominance of either micro-trips or long high-speed segments during Monte Carlo reconstruction, the trip library is standardized using a 10-min target scale. Consecutive trips from the same operating mode are merged if their combined duration does not exceed 10 min, and any trip longer than 10 min is split into two approximately equal sub-trips. The 10-min threshold is an empirical standardization scale for trajectory libraries rather than a regulatory prerequisite or WHTC sub-phase duration. It reduces the numerical dominance of very short urban fragments and the duration/work dominance of long rural or motorway fragments. Importantly, duration equalization modifies only the sampling-unit definition; all second-by-second speed, power, temperature, and NOx records are retained for subsequent MAW calculations.

Stage 3 performs Monte Carlo simulation and synthetic cycle reconstruction. For a given evaluation period, synthetic driving cycles are iteratively constructed through stochastic sampling until a valid cycle satisfying all reference constraints is obtained. The process begins by initializing an empty cycle and defining target phase durations based on the regulatory proportions and a randomly selected total-work multiplier β drawn from a uniform distribution over the interval of 4–7. Cycle construction then proceeds sequentially in the prescribed order of urban, rural, and motorway operation. Within each phase, trips are randomly sampled without replacement from the corresponding mode-specific library and appended until the cumulative phase duration reaches or exceeds its target value. Once all three phases have been assembled, the average speed of each phase and total cumulative work are calculated. If all phase-share, phase-speed, driving-order, and work-multiplier constraints are satisfied, the cycle is accepted; otherwise, it is discarded and reconstruction restarts. This rejection-sampling procedure ensures that every retained synthetic cycle is individually compatible with the applicable China VI reference requirements.

Stage 4 applies the MAW calculation and aggregates the reconstructed indicator. For each successfully generated synthetic cycle, the standard MAW method described in Section 2.3 is executed in full, yielding one SE_{NOx}_P90 value. Stages 3 and 4 are independently repeated N_{MC} times for the same evaluation period, producing an ensemble of SE_{NOx}_P90 estimates. The final reconstructed indicator for the period is defined as the median of this ensemble. Median-based aggregation

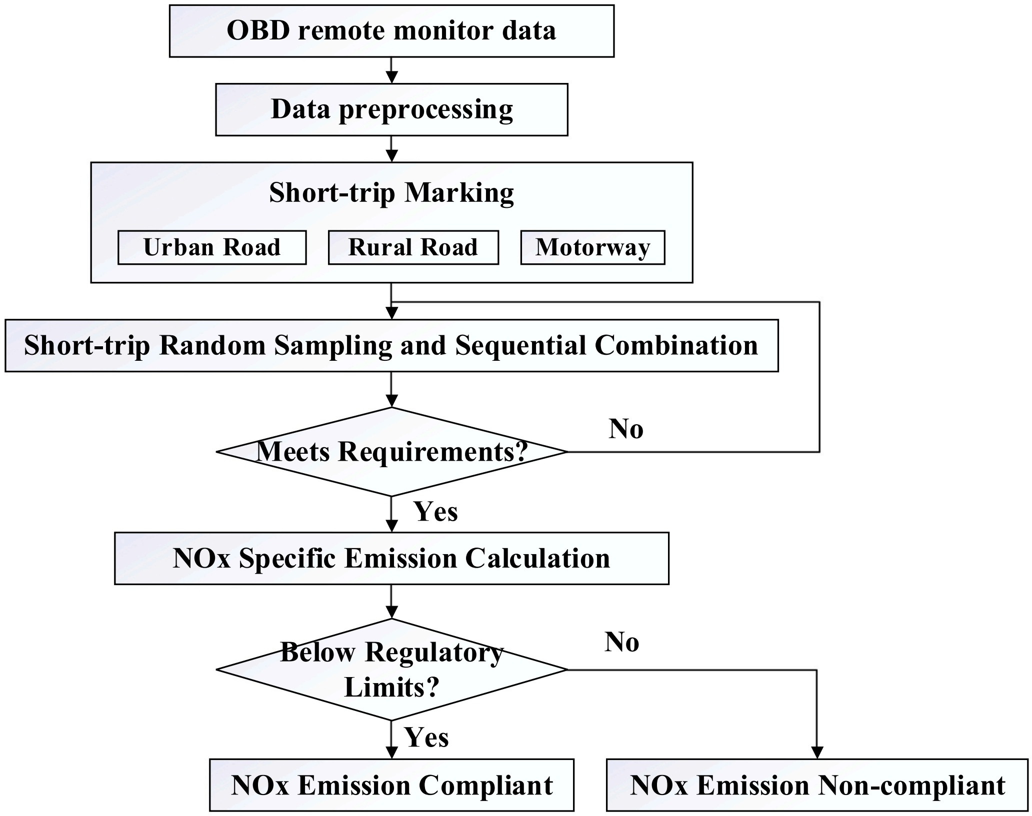

Fig. 5. Complete workflow of the STCM.

reduces sensitivity to extreme sampling outcomes and sequence-dependent effects that can occur when a small number of high-emission fragments are positioned inside or outside valid MAW windows.

3. Key parameter analysis and optimization

To ensure the robustness and reliability of the STCM framework for practical fleet-scale application, three key operational parameters were systematically evaluated and optimized. These parameters determine the trade-offs among assessment timeliness, data representativeness, computational efficiency, and the robustness of the final indicator reconstruction.

3.1. *Determination of the evaluation period (Data window length)*

The selection of the evaluation period involves a fundamental trade-off between assessment timeliness and data sufficiency. A shorter window enables more frequent indicator updates and more rapid detection of emission deterioration or tampering, but may not adequately capture the diversity of real-world vehicle operation. By contrast, a longer window enhances data representativeness but delays the identification of persistently elevated emissions and increases computational burden. To define this parameter on a pragmatic data-driven basis, an empirical trip-sample adequacy criterion was introduced: within a given evaluation period, the number of available trip fragments for each road type should be at least three times the minimum number required to assemble a compliant minimum-duration RDE test. This factor ensures sufficient diversity in the trip library for statistically robust Monte Carlo resampling while avoiding excessive sensitivity to limited data availability.

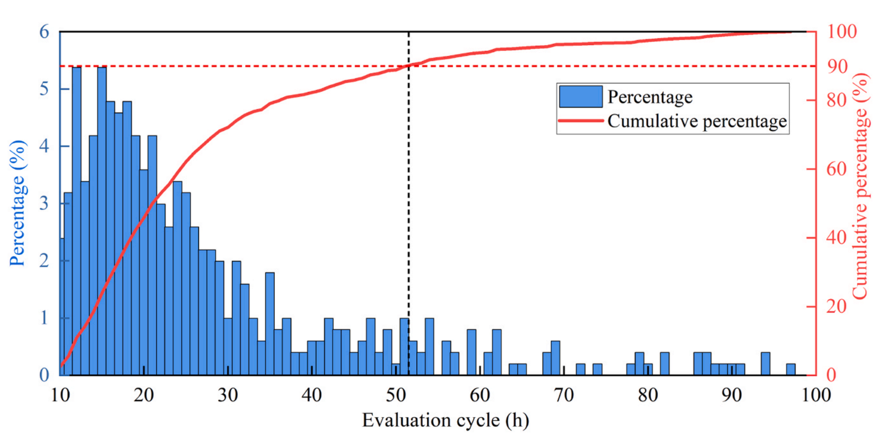

Fig. 6. Cumulative distribution function of the minimum data duration required to satisfy STCM trip sample adequacy criteria for 502 heavy-duty diesel vehicles.

Based on the full fleet of 502 vehicles, the minimum data duration, expressed in cumulative engine operating hours, required to satisfy this criterion was determined for each vehicle. Fig. 6 presents the cumulative distribution of these minimum required durations. The distribution is right-skewed, indicating that most vehicles accumulated adequate short-trip diversity within relatively short operating times, whereas a minority required substantially longer observation because of repetitive or constrained duty cycles. To establish a conservative and uniform benchmark applicable to more than 90% of the fleet, a standard evaluation period of 51 h of cumulative engine operation was selected. For vehicles that still fail the trip-diversity criterion after 51 h, a standard STCM result should not be forced. Instead, they should be flagged as having insufficient operational diversity, monitored over an extended window, or evaluated using a duty-specific protocol when their operation is inherently constrained.

3.2. Robustness verification of synthetic cycle length (Cumulative work multiplier)

RDE regulations require the total cumulative engine work of a valid test to fall within the range of 4–7 times W_{ref}. Although this provision offers flexibility in total test duration, it may also introduce variability in emission outcomes because longer tests can contain additional low-emission high-speed operation. To evaluate the sensitivity of STCM to this parameter, a controlled comparison was conducted with Vehicle A. Two RDE tests were performed on consecutive days under similar traffic and ambient conditions but with different cumulative-work levels: 4.5 W_{ref} and 6.4 W_{ref}, respectively. Fig. 7 compares the corresponding vehicle-speed profiles and instantaneous NOx emission rates.

As shown in Fig. 8, extending the cycle length increased the number of valid MAW windows, with most additional windows occurring in the motorway phase. Because sustained high exhaust temperatures during motorway operation favor high SCR conversion efficiency, these additional windows exhibited very low specific NOx emissions. Consequently, the mean specific NOx emission across valid windows decreased from 0.138 g/kWh in the shorter test to 0.123 g/kWh in the longer test, a relative decrease of approximately 10.8%. In contrast, SE_{NOx}_P90 decreased only marginally, from 0.190 to 0.183 g/kWh, a change of less than 4% (Fig. 9). This limited response reflects the upper-tail nature of SE_{NOx}_P90. High-emission windows are typically associated with transient events during nominally hot operation, such as urban stop-and-go driving, after-treatment temperature excursions, rapid load increases, or aggressive acceleration. Once these high-emission events are represented in the trip library, adding additional low-emission motorway windows has limited influence on the 90th percentile. These results indicate that STCM is not unduly sensitive to reasonable variation in synthetic-cycle length, provided that the trip library captures the main high-emission operating modes. Accordingly, the target cumulative-work multiplier β was sampled uniformly from the interval of 4–7 to reflect the admissible reference range while increasing reconstruction diversity.

3.3. Optimization of Monte Carlo resampling iterations

Within each evaluation period, the trip library contains numerous short trips, and their emission characteristics can vary substantially even within the same driving mode. This intra-mode variability arises from differences in traffic congestion, road grade, driver behavior, payload, and the thermal state of the after-treatment system at trip onset. A single random sampling event may therefore produce an SE_{NOx}_P90 estimate that deviates from the central tendency of the vehicle's emission behavior. The sequential ordering of trips introduces another source of variability. As illustrated in Fig. 10, valid MAW windows are not uniformly distributed throughout a driving cycle. Because of the APR validation criterion, windows with higher average power are more likely to be valid. In a typical RDE-compliant cycle following the prescribed urban-rural-motorway sequence, many valid windows occur in the latter part of the test, where higher-speed and higher-load operation dominates. Consequently, high-emission urban fragments placed near the beginning of the cycle may be underrepresented in the valid-window set, whereas similar fragments positioned within valid windows may increase the reconstructed P90. This ordering effect introduces stochastic noise that must be mitigated through repeated sampling and robust aggregation.

To mitigate the combined influences of sampling variability and ordering sensitivity, STCM employs multi-iteration resampling, with the final NOx indicator defined as the median of the SE_{NOx}_P90 distribution obtained from independent Monte Carlo simulations. To determine the appropriate number of iterations, a convergence analysis was conducted using data from multiple vehicles. As shown in Fig. 11 for Vehicle A, the median SE_{NOx}_P90 fluctuated considerably at low iteration numbers but gradually stabilized as N_{MC} increased. When $N_{MC} = 200$, the fluctuation range of the median SE_{NOx}_P90 decreased to less than 0.035 g/kWh, corresponding to approximately 5% of the China VI reference value (0.69 g/kWh). Further increasing N_{MC} yielded only marginal stability gains while increasing computational cost. Similar convergence

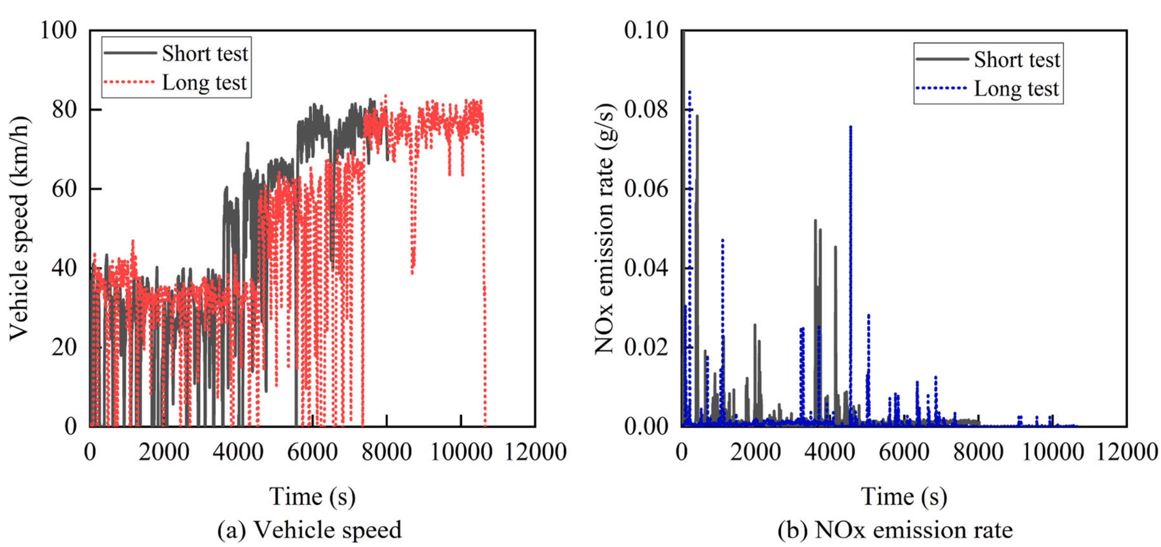

Fig. 7. Comparison of vehicle speed and instantaneous NOx emission rate between short-duration ($4.5W_{ref}$) and long-duration ($6.4W_{ref}$) RDE tests conducted on adjacent days.

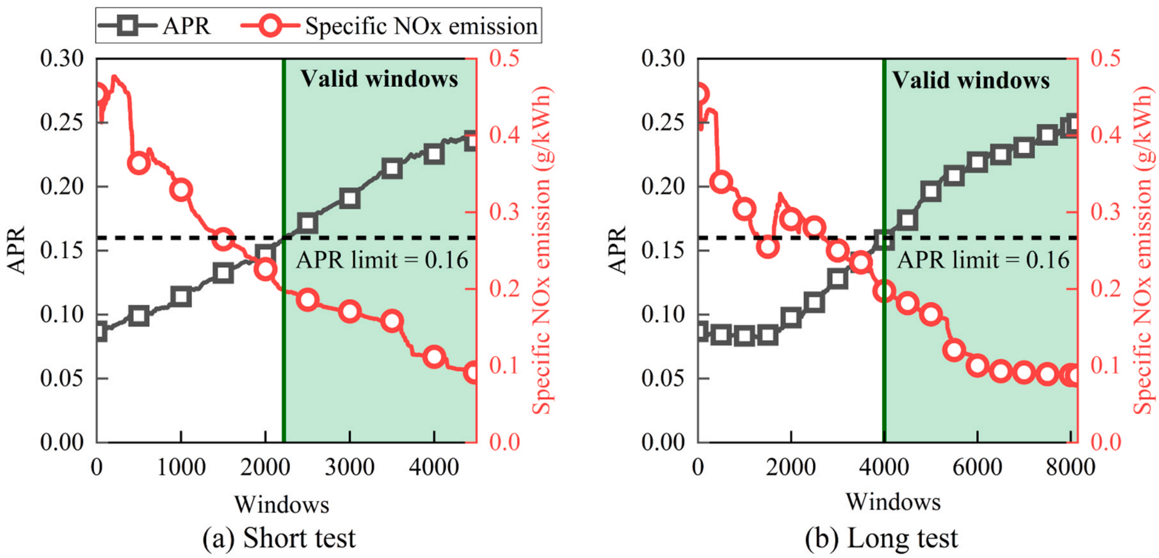

Fig. 8. Comparison of valid MAW window distribution between short test and long test.

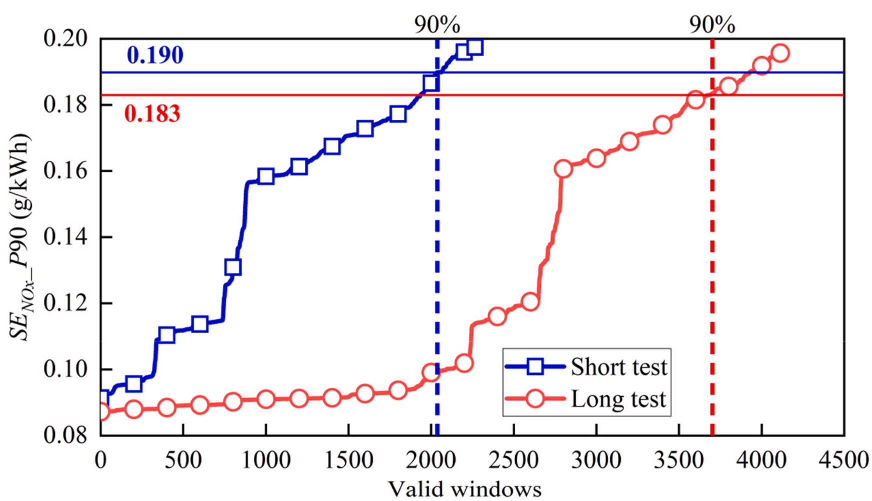

Fig. 9. Comparison of SE_{NOx}_P90 values between short test and long test.

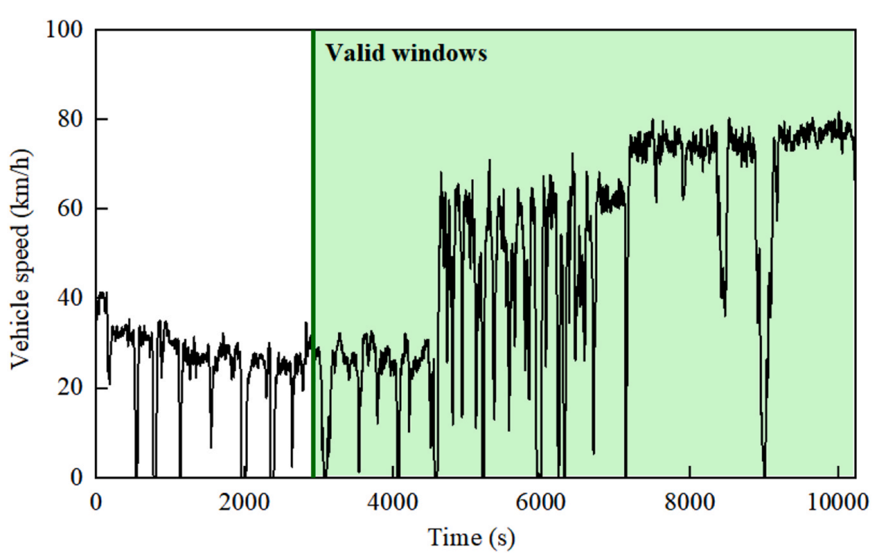

Fig. 10. Schematic illustration of the valid windows distribution.

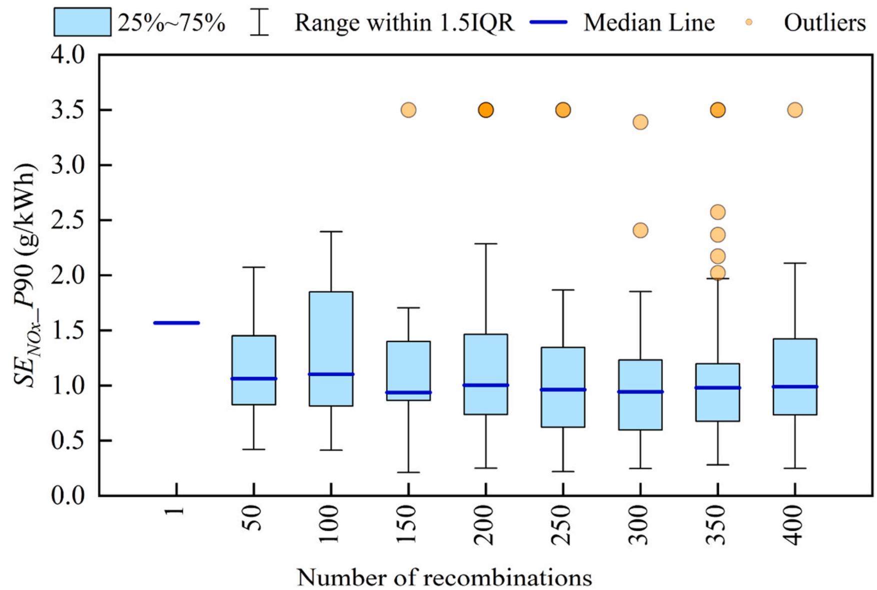

Fig. 11. Convergence of the median SE_{NOx}_P90 estimate as a function of the number of Monte Carlo iterations for vehicle A.

behavior was observed for the other three test vehicles. Accordingly, $N_{MC} = 200$ was selected as the standard configuration, balancing robustness and computational efficiency.

This computational configuration is also compatible with large-scale fleet screening. In our implementation, using a workstation equipped with an AMD EPYC 7H12 CPU and 128 GB RAM, processing all 502 vehicles required approximately 55 s after completion of raw-data quality control. This runtime corresponds to an approximate throughput of 0.8 million vehicle-level evaluations per day under similar batch-processing conditions. The value is an implementation-specific estimate rather than a universal benchmark, but it indicates that the STCM workflow is computationally feasible for routine remote-monitoring applications.

4. Results and validation analysis

4.1. Fleet-scale reconstructed NOx distribution

To demonstrate the value of the complete telematics dataset, STCM was first applied to the 502-vehicle fleet using May 2023 as an illustrative fleet-screening period. The reconstructed hot-running SE_{NOx}_P90 values showed substantial between-vehicle heterogeneity (Fig. 12), indicating that long-duration OBD telematics can identify vehicles with persistently elevated NOx behavior that may be missed by sparse spot inspections. The vehicle-category distributions also indicate that the reconstructed indicator reflects both technology and duty-cycle differences rather than a single fleet-wide average. Interpreted against the China VI reference value of 0.69 g/kWh for screening purposes, 15.9% of the 502 vehicles were flagged as elevated hot-running NOx emitters, corresponding to approximately 65 vehicles. Among these flagged vehicles, 31% had OBD-reported NOx-control-related faults, such as injector blockage or abnormal urea-consumption deviation. This association should not be interpreted as component-level diagnosis, because OBD faults and reconstructed emissions do not have one-to-one correspondence. Nevertheless, it demonstrates that STCM can transform routine telematics into an environmentally meaningful prioritization tool for identifying vehicles or operating periods requiring confirmatory inspection.

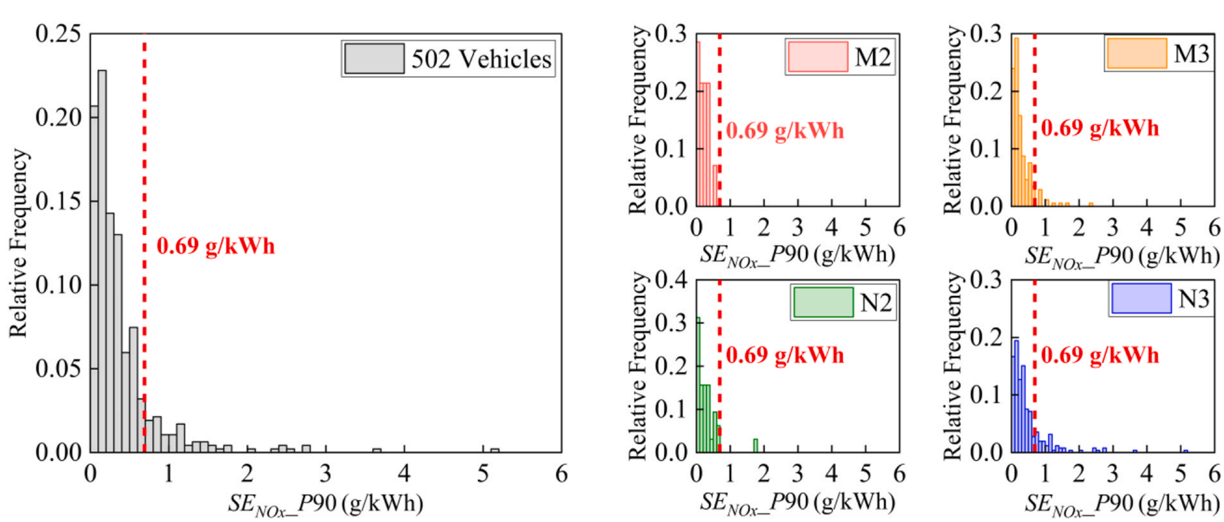

Fig. 12. Fleet-scale distribution of reconstructed hot-running SE_{NOx}_P90 values for the 502-vehicle telematics dataset, stratified by vehicle category and interpreted relative to the China VI reference value.

4.2. PEMS benchmark validation

For proof-of-concept benchmark validation, a sliding-window protocol was adopted for the four PEMS-tested vehicles. Based on the 51 h evaluation window established in Section 3.1, overlapping assessment windows were sequentially extracted with a sliding step of 10 h of cumulative engine operation. This protocol simulates a continuous monitoring scenario in which the vehicle-specific hot-running NOx indicator is periodically updated using the most recent 51 h of operation. For each extracted window, STCM was applied with 200 Monte Carlo iterations, and the final indicator was defined as the median SE_{NOx}_P90 of the simulated distribution. In parallel, PEMS data collected for each vehicle served as the benchmark reference; the corresponding PEMS SE_{NOx}_P90 values were calculated using the standard MAW method. A simple whole-trip average, calculated from the same quality-controlled hot-running OBD records but without regulation-constrained reconstruction or MAW window validation, was also evaluated as a baseline. Detailed vehicle-level values and summary metrics are provided in Supplementary Tables S3 and S4.

Fig. 13 shows that the STCM median generally agrees with the central tendency of repeated PEMS measurements. Across the four vehicles, the vehicle-level absolute errors between STCM and the PEMS mean ranged from 0.110 to 0.182 g/kWh, with an overall MAE of 0.133 g/kWh and RMSE of 0.136 g/kWh (Supplementary Table S4). The exploratory R^2 between STCM and PEMS means was 0.899, whereas whole-trip averaging yielded a substantially larger MAE of 0.277 g/kWh, RMSE of 0.381 g/kWh, and exploratory R^2 of 0.208 (Fig. 14 and Supplementary Table S4). These results show that the improved agreement is not simply the result of averaging more OBD data; it arises from reconstructing MAW-compatible cycles and preserving valid-window logic. Vehicles C and D exhibited larger STCM spreads than Vehicles A and B. Supplementary Figs. S1-S3 indicate that this spread is consistent with greater temporal variability in road-type composition and after-treatment thermal behavior. In particular, the supplementary SCR-

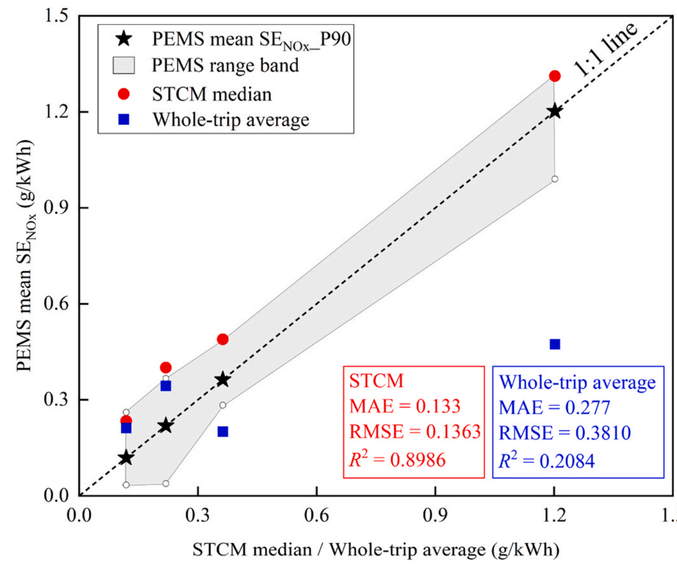

Fig. 14. Comparison of STCM-derived and whole-trip average indicators against PEMS measurements.

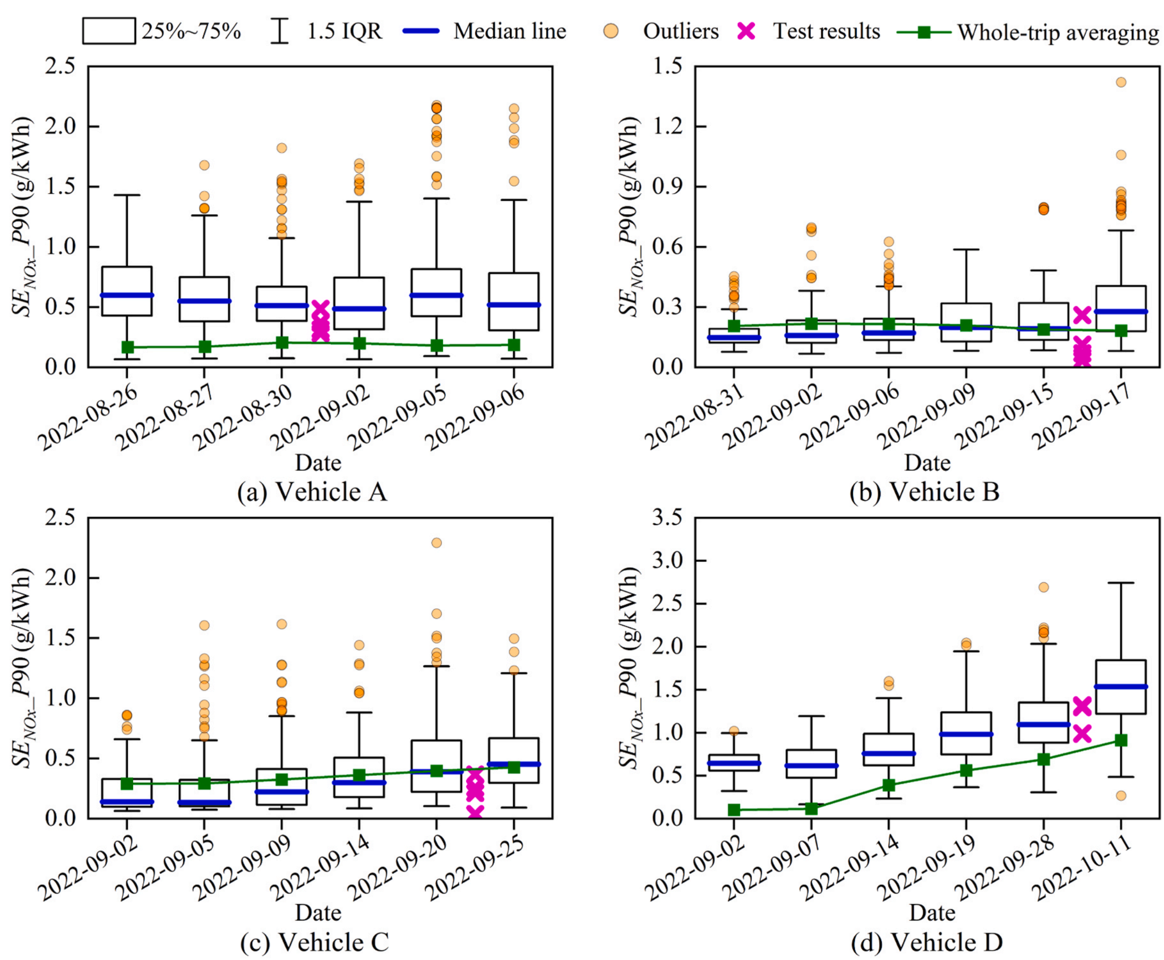

Fig. 13. Validation of STCM-derived SE_{NOx}_P90 estimates against repeated PEMS benchmark measurements.

temperature and SCR-efficiency trends show stronger thermal and conversion-efficiency variation for Vehicle D, while Vehicle C shows greater variation in route composition than the more stable commuter pattern of Vehicle B. Therefore, the wider STCM distributions are interpreted as reflecting heterogeneous real-world operation and after-treatment thermal states rather than Monte Carlo numerical instability alone. Direct component-level diagnosis was not available, so possible contributions from after-treatment deterioration and onboard NOx sensor behavior are discussed as uncertainty sources rather than asserted as confirmed causes.

5. Discussion

5.1. Methodological significance for real-world NOx monitoring

The principal contribution of STCM is not merely methodological reconstruction of a regulation-compatible indicator, but the recovery of environmentally relevant long-duration NOx behavior from fragmented routine telematics. Existing in-use emission assessment methods are either accurate but sparse, as in PEMS-based testing, or scalable but weakly suited to capturing long-duration elevated-emission behavior. STCM addresses this methodological gap by converting fragmented operational telemetry into a form that remains comparable to a reference window-based framework while preserving the diversity of real-world operation. In this sense, the framework extends the practical use of routine OBD monitoring from passive data collection to environmentally relevant reconstruction of in-use NOx behavior. This is environmentally important because persistent or intermittent high-emission behavior may be systematically missed by sparse spot testing yet may still contribute disproportionately to roadside NOx exposure and regional precursor loading.

A second methodological strength of STCM lies in its explicit treatment of real-world variability. Vehicle operation in normal service is intrinsically stochastic, and any attempt to define a single "representative" trip is therefore vulnerable to arbitrariness. STCM addresses this issue by adopting a Monte Carlo reconstruction strategy, generating an ensemble of plausible synthetic cycles rather than relying on a single deterministic realization. The final use of the median SE_{NOx}_P90 further enhances robustness by reducing the influence of atypical sampling outcomes and sequence-dependent effects. This is particularly important in the present context, because the upper-tail emission metric is governed by the upper tail of the emission distribution rather than by average emission behavior. Accordingly, the framework is designed to characterize the central tendency of in-use emission behavior while remaining resistant to extreme but non-representative cycle constructions.

The validation results indicate that this methodological design is robust across the tested vehicles and operating conditions. For all four vehicles, the median STCM-derived SE_{NOx}_P90 fell within the range of repeated PEMS measurements, despite substantial variability in real-world test results. This finding suggests that STCM can reproduce the central tendency of vehicle emission performance as characterized by the regulatory reference method, while drawing on a much larger and more diverse operational dataset. Additional support for robustness is provided by the sensitivity analysis of total cycle length: although extending the cycle from $4.5W_{ref}$ to $6.4W_{ref}$ reduced mean NOx emissions by 10.8%, the corresponding change in SE_{NOx}_P90 remained below 4%. This result confirms that the STCM outcome is driven primarily by the occurrence of high-emission events, rather than by the inclusion of additional low-emission motorway operation, and is therefore not unduly sensitive to reasonable variation in synthetic cycle construction.

The interpretation of SE_{NOx}_P90 should nevertheless be distinguished from mean emission intensity or total NOx mass. P90 is intentionally sensitive to the upper tail of the valid-window distribution and is therefore suitable for identifying elevated-emission behavior and prioritizing vehicles for confirmatory inspection. It should not be used alone to quantify the total emission inventory. The hot-running scope of the present indicator also requires careful interpretation. Cold-start and SCR warm-up phases may contribute substantially to the total real-world NOx burden, especially for vehicles with frequent restarts, short trips, or prolonged low-temperature operation. Excluding these phases can underestimate total trip-level emissions. This choice was made to preserve comparability with the China VI/RDE MAW evaluation boundary rather than to claim full inventory coverage. A future monitoring framework should therefore combine the present hot-running STCM indicator with a dedicated cold-start/warm-up sub-indicator.

5.2. Sources of uncertainty and limitations

Despite its methodological advantages, STCM's performance remains fundamentally constrained by the quality of the underlying OBD telemetry. As with any remote-monitoring-based approach, the reliability of the final reconstructed indicator depends on the accuracy and stability of the onboard measurements used to derive NOx mass emissions, including NOx sensor signals, exhaust-flow estimation, and relevant engine operating parameters. In SCR-equipped vehicles, ammonia slip may introduce NH_3 cross-sensitivity in downstream NOx sensors, and transient exhaust conditions or sensor drift may further bias the reported signal [30]. STCM does not eliminate this sensor-level uncertainty; rather, it propagates the available OBD measurements through a structured MAW-compatible reconstruction framework. Practical deployment should therefore include sensor-quality diagnostics, cross-checks between upstream and downstream NOx signals, SCR temperature and urea-dosing plausibility checks, and, where possible, NH_3-bias correction before the reconstructed indicator is used for regulatory-scale screening [19].

A second limitation concerns the representativeness of the operational data window. Although the 51-h evaluation period was selected to ensure adequate trip diversity for most vehicles, the approach may be less suitable for vehicles with highly repetitive or operationally constrained duty cycles. In such cases, the trip library may not contain sufficient variability to support meaningful cycle reconstruction, even if the nominal data volume is adequate. This issue is particularly relevant for specialized vehicles operating predominantly in confined areas or under atypical load patterns. The current framework is therefore best suited to vehicles with sufficiently diverse on-road activity, and its applicability to highly homogeneous operating regimes remains limited.

The scope of validation also requires careful qualification. The present study was conducted on four China VI-compliant diesel vehicles equipped with modern DOC-DPF-SCR-ASC after-treatment systems. Although these vehicles exhibited different real-world operating patterns, they do not represent the full diversity of the in-service fleet. The transferability of STCM to older emission standards, alternative after-treatment architectures, hybridized powertrains, or non-road applications has not yet been established. Accordingly, the present results should be interpreted as evidence of feasibility and robustness within the tested application domain, rather than as universal validation across all vehicle categories.

5.3. Environmental implications and practical application

From an environmental perspective, the main value of STCM lies in extending routine OBD telematics from operational reporting to long-duration screening of real-world NOx burden. This is particularly relevant because elevated NOx emissions can be intermittent and thermally sensitive, making them difficult to capture with sparse spot measurements. By converting fragmented telematics into stable indicators, the framework can support earlier identification of vehicles or operating periods associated with persistently elevated emissions, improve fleet-scale characterization of real-world NOx behavior, and help prioritize confirmatory inspection resources toward environmentally relevant high-emission cases. When interpreted relative to the China VI reference value of 0.69 g/kWh, the reconstructed SE_{NOx}_P90 can serve as a screening reference for identifying vehicles or operating periods with potentially elevated hot-running NOx behavior. This comparison should not be used as a formal compliance decision without confirmatory PEMS testing.

Practical application of the framework will nevertheless require improved quality assurance for onboard NOx data, particularly with respect to sensor drift, cross-sensitivity, and anomalous measurements. Broader validation across vehicle technologies, duty cycles, and sensing conditions is also needed before large-scale deployment. These next steps are essential for determining how telematics-based reconstruction can be integrated into future environmental monitoring of in-use vehicle emissions.

6. Conclusion

This study developed and evaluated the STCM for reconstructing a hot-running, MAW-compatible SE_{NOx}_P90 indicator from irregular OBD data of HDDVs. Using 13 months of telematics data from 502 China VI vehicles, the analysis indicated that a 51-h evaluation window provided sufficient trip diversity for most vehicles and that 200 Monte Carlo iterations yielded stable indicator estimates. Fleet-level application to the 502-vehicle dataset showed substantial between-vehicle heterogeneity and flagged 15.9% of vehicles as elevated hot-running NOx emitters when interpreted against the China VI reference value of 0.69 g/kWh for screening purposes. Among the flagged vehicles, 31% had OBD-reported NOx-control-related faults, supporting the practical value of STCM for prioritizing confirmatory inspection. Proof-of-concept benchmark comparison against 15 PEMS tests on four representative vehicles showed that the STCM median generally fell within the range of repeated PEMS measurements, with vehicle-level absolute errors of 0.110–0.182 g/kWh, MAE of 0.133 g/kWh, RMSE of 0.136 g/kWh, and exploratory R^2 of 0.899. Controlled comparison of 4.5 W_{ref} and 6.4 W_{ref} test conditions further suggested limited sensitivity of the reconstructed indicator to reasonable variation in synthetic-cycle length.

Taken together, these findings show that irregular long-duration OBD telematics can be transformed into environmentally relevant hot-running NOx indicators for screening-oriented assessment of in-use emission behavior. The framework is best interpreted as a complement to, rather than a replacement for, PEMS, with practical value in identifying persistently elevated-emission vehicles or operating periods that warrant confirmatory inspection. The present study remains limited by the small PEMS validation sample, exclusion of cold-start and SCR warm-up operation, dependence on onboard sensing quality, and untested transferability to some vehicle categories such as N2 vehicles and specialized duty cycles. Future work should expand external validation, develop complementary cold-start indicators, strengthen telematics data quality assurance, and evaluate broader deployment across more diverse in-use fleets.

Environmental implication

Heavy-duty diesel vehicles remain an important in-use source of atmospheric NOx, and persistent high-emission behavior is often difficult to capture using sparse spot measurements. This study provides a practical framework for reconstructing environmentally relevant NOx indicators from irregular OBD telematics, enabling continuous fleet-scale screening under real-world operating conditions. By improving identification of persistently elevated emitters and abnormal operating periods, the proposed method can support more targeted inspection and maintenance, strengthen in-use emissions surveillance, and enhance the environmental value of routine digital monitoring for reducing road-transport-related air pollution.

CRediT authorship contribution statement

Chuntao Liu: Writing – original draft, Visualization, Software, Investigation, Data curation. **Chunling Wu:** Resources, Investigation, Funding acquisition. **Yiqiang Pei:** Supervision, Project administration, Funding acquisition. **Dasuo Yao:** Writing – review & editing, Methodology, Investigation. **Zhiqiang Li:** Writing – review & editing, Methodology, Investigation. **Chenxi Wang:** Writing – review & editing, Validation, Methodology, Formal analysis, Conceptualization.

Declaration of Competing Interest

The authors declare that they have no known competing financial interests or personal relationships that could have appeared to influence the work reported in this paper.

Acknowledgement

This work was financially supported by the Key Technologies Research and Development Program (China) (Grant Nos. 2022YFC3701805 and 2022YFC3703600) and technically supported by the CATARC Automotive Test Center Company Limited (Tianjin). The authors sincerely thank Guomin Pang and Weilin Liu of the CATARC Automotive Test Center Company Limited for their significant contributions to this program's emissions testing and data collection activities.

Appendix A. Supporting information

Supplementary data associated with this article can be found in the online version at doi:10.1016/j.jhazmat.2026.142913.

Data availability

The authors do not have permission to share data.

References

[1] European Environment Agency. Sustainability of Europe's mobility systems 2024: Air pollution. European Environment Agency; 2024. Accessed 24 May 2026.
[2] Kazemi Bakhshmand, S., Mulholland, E., Tietge, U., et al., 2022. Remote sensing of heavy-duty vehicle emissions in Europe. ICCT Working Paper 2022-25. International Council on Clean Transportation, Washington, DC.
[3] Anenberg, S.C., Miller, J., Minjares, R., et al., 2017. Impacts and mitigation of excess diesel-related NOx emissions in 11 major vehicle markets. Nature 545, 467–471. https://doi.org/10.1038/nature22086.
[4] Ke, J., Jiang, H., Yang, X., et al., 2025. Evaluation of real-world CO_2 and NOx emissions of various in-use heavy-duty vehicles. J Hazard Mater 496, 139243. https://doi.org/10.1016/j.jhazmat.2025.139243.
[5] Wang, Z., Acha, S., Bird, M., et al., 2024. A total cost of ownership analysis of zero emission powertrain solutions for the heavy goods vehicle sector. J Clean Prod 434, 139910. https://doi.org/10.1016/j.jclepro.2023.139910.
[6] He, L., Li, G., Wu, X., et al., 2024. Characteristics of NOx and NH_3 emissions from in-use heavy-duty diesel vehicles with various aftertreatment technologies in China. J Hazard Mater 465, 133073. https://doi.org/10.1016/j.jhazmat.2023.133073.
[7] McCaffery, C., Zhu, H., Tang, T., et al., 2021. Real-world NOx emissions from heavy-duty diesel, natural gas, and diesel hybrid electric vehicles of different vocations on California roadways. Sci Total Environ 784, 147224. https://doi.org/10.1016/j.scitotenv.2021.147224.
[8] Jiang, Y., Tan, Y., Yang, J., et al., 2022. Understanding elevated real-world NOx emissions: Heavy-duty diesel engine certification testing versus in-use vehicle testing. Fuel 307, 121771. https://doi.org/10.1016/j.fuel.2021.121771.
[9] Hao, L., Zhao, Z., Yin, H., et al., 2022. Study of durability of diesel vehicle emissions performance based on real driving emission measurement. Chemosphere 297, 134171. https://doi.org/10.1016/j.chemosphere.2022.134171.
[10] Giechaskiel, B., Forloni, F., Carriero, M., et al., 2022. Effect of tampering on on-road and off-road diesel vehicle emissions. Sustainability 14, 6065. https://doi.org/10.3390/su14106065.
[11] Tian, M., He, L., Peng, D., et al., 2024. Characterizing NOx emissions from diesel trucks with tampered aftertreatment systems and its implications for identifying high emitters. Sci Total Environ 917, 170378. https://doi.org/10.1016/j.scitotenv.2024.170378.
[12] Chen, L., Wang, Z., Liu, S., et al., 2018. Using a chassis dynamometer to determine the influencing factors for the emissions of Euro VI vehicles. Transp Res Part D Transp Environ 65, 564–573. https://doi.org/10.1016/j.trd.2018.09.022.

[13] Van Niekerk, A.S., Drew, B., Larsen, N., et al., 2019. Influence of blends of diesel and renewable fuels on compression ignition engine emissions over transient engine conditions. Appl Energy 255, 113890. https://doi.org/10.1016/j.apenergy.2019.113890.
[14] Liu, C., Pei, Y., Wu, C., et al., 2025. The impact of the variation in driving conditions on the NOx emissions characteristics in PEMS test for heavy-duty vehicle. J Eng Res 13, 294–301. https://doi.org/10.1016/j.jer.2023.10.024.
[15] Tong, Z., Li, Y., Lin, Q., et al., 2022. Uncertainty investigation of plume-chasing method for measuring on-road NOx emission factors of heavy-duty diesel vehicles. J Hazard Mater 424, 127372. https://doi.org/10.1016/j.jhazmat.2021.127372.
[16] Yang, Z., Tate, J.E., Rushton, C.E., et al., 2022. Detecting candidate high NOx emitting light commercial vehicles using vehicle emission remote sensing. Sci Total Environ 823, 153699. https://doi.org/10.1016/j.scitotenv.2022.153699.
[17] Zhao, J., Peng, L., Zhu, G., et al., 2026. Emission-trend-constrained quality assessment model for remote sensing data of vehicle NO emissions. J Hazard Mater 505, 141416. https://doi.org/10.1016/j.jhazmat.2026.141416.
[18] Shen, X., Yao, Z., Zhang, Q., et al., 2015. Development of database of real-world diesel vehicle emission factors for China. J Environ Sci 31, 209–220. https://doi.org/10.1016/j.jes.2014.10.021.
[19] Liu, C., Wang, C., Li, Z., et al., 2026. NH_3 slip identification and NH_3-induced bias correction in remote NOx emissions monitoring of heavy-duty diesel vehicles. J Environ Manag 404, 129576. https://doi.org/10.1016/j.jenvman.2026.129576.
[20] Wu, Y., Sperling, D., 2018. Using on-board diagnostic and global positioning system to price emissions from on-road heavy-duty vehicles. J Transp Eng Part A Syst 144, 04018041. https://doi.org/10.1061/JTEPBS.0000167.
[21] Wang, C., He, K., Fang, X., et al., 2020. Design and implementation of emission monitoring platform for heavy-duty diesel vehicles. Proceedings of the 2020 International Conference on Computer Science and Management Technology, pp. 336–339.
[22] Ge, Y., Hou, P., Lyu, T., et al., 2023. Machine learning-aided remote monitoring of NOx emissions from heavy-duty diesel vehicles based on OBD data streams. Atmosphere 14, 651. https://doi.org/10.3390/atmos14040651.
[23] Ministry of Ecology and Environment of the People's Republic of China. Technical specification for emission remote supervision system of heavy-duty vehicles—Part 3: Communication protocol and data format, HJ 1239.3-2021. Beijing: China Environmental Science Press; 2021. In Chinese.
[24] Mendoza-Villafuerte, P., Suarez-Bertoa, R., Giechaskiel, B., et al., 2017. NOx, NH_3, N_2O and PN real driving emissions from a Euro VI heavy-duty vehicle. Impact of regulatory on-road test conditions on emissions. Sci Total Environ 609, 546–555. https://doi.org/10.1016/j.scitotenv.2017.07.168.
[25] Du, B., Zhang, L., Geng, Y., et al., 2020. Testing and evaluation of cold-start emissions in a real driving emissions test. Transp Res Part D Transp Environ 86, 102447. https://doi.org/10.1016/j.trd.2020.102447.
[26] Liu, C., Pei, Y., Wu, C., et al., 2023. Novel insights into the NOx emissions characteristics in PEMS tests of a heavy-duty vehicle under different payloads. J Environ Manag 348, 119400. https://doi.org/10.1016/j.jenvman.2023.119400.
[27] Barbier, A., Salavert, J.M., Palau, C.E., et al., 2024. Analysis of the Euro 7 on-board emissions monitoring concept with real-driving data. Transp Res Part D Transp Environ 127, 104062. https://doi.org/10.1016/j.trd.2024.104062.
[28] Wang, J., Wang, R., Yin, H., et al., 2022. Assessing heavy-duty vehicles (HDVs) on-road NOx emissions in China from on-board diagnostics (OBD) remote report data. Sci Total Environ 846, 157209. https://doi.org/10.1016/j.scitotenv.2022.157209.
[29] Ministry of Ecology and Environment of the People's Republic of China, State Administration for Market Regulation. Limits and measurement methods for emissions from diesel-fueled heavy-duty vehicles (China VI), GB 17691-2018. Beijing: China Environmental Science Press; 2018. In Chinese.
[30] Funk, S., 2021. Real world NOx sensor accuracy assessment and implications for real NOx tracking. SAE Int J Adv Curr Pract Mobil 3, 2761–2769. https://doi.org/10.4271/2021-01-0593.